

# Kinetics of voltage-induced conductance increases in the outer mitochondrial membrane

Kathleen W. Kinnally,\* Henry Tedeschi,\* Carmen A. Mannella,<sup>†</sup> and Harry L. Frisch<sup>§</sup>

Departments of \*Biological Sciences and <sup>§</sup>Chemistry, State University of New York at Albany, Albany, New York 12222; and <sup>†</sup>Wadsworth Center for Laboratories and Research, New York State Department of Health, Albany, New York 12201

**ABSTRACT** The kinetics of the increase in conductance in the outer mitochondrial membrane induced by patch-clamping at various negative potentials (pipette inside negative) are reported.

The changes are biphasic, a rapid increase is followed by a slowly developing larger change. The results can be predicted by a model in which an initial activation of channels is followed

by their assembly into highly conducting channels. The model suggests that five to seven activated subunits form each high-conductance channel.

## INTRODUCTION

The channels of the outer mitochondrial membrane have been studied primarily by reconstituting extracts with phospholipid bilayers. A mitochondrial outer membrane protein of ~30 kD forms a voltage-dependent, anion-selective channel (VDAC or mitochondrial porin). The reconstituted channel with a conductance of ~4.5 nS in 1 M KCl exhibits a much lower conductance, ~2.4 nS, with voltage in the range of 20–50 mV regardless of polarity (Colombini, 1985; Benz, 1985; De Pinto et al., 1987). More recently, Thieffry et al. (1988) have observed a mitochondrial channel incorporated into phospholipid bilayers on a patch-pipette tip. In 150 mM NaCl, the channel exhibits four conductance levels separated by transitions of 0.1, 0.22, and another of 0.22 nS. The channel has been found to have a slight cationic selectivity. Although the site of the channel is now known, a location in the outer membrane is possible because membranes of whole mitochondria were used. Sorgato et al. (1987) reported a single channel with conductance of 0.35 nS in 150 mM KCl, which may correspond to the VDAC. This channel was observed by patch-clamping intact mitochondria.

We have applied patch-clamp techniques to the intact outer membrane of giant mitochondria (Tedeschi et al., 1987; Kinnally et al., 1987) and vesicles derived from *Neurospora* outer membranes (Tedeschi et al., 1987). Consistent with the expected high concentration of channels in the outer mitochondrial membrane (Freitag et al., 1982), the patches have relatively low resistance, typically in the range of 10–500 Mohms in 10 mM KCl. The conductances computed from the macroscopic current records vary with voltage. When the potential is positive in relation to the patch pipette,<sup>1</sup> the conductance decreases with increased magnitude of the voltage, a behavior analogous to that of VDAC incorporated into

bilayers. In accordance with this view, the voltage-dependent decrease in conductance is sensitive to the presence of polyanions and treatment with succinic anhydride, both of which similarly affect VDAC. Under the conditions used the former increases (Colombini et al., 1987) and the latter decreases (Doring and Colombini, 1985) the voltage sensitivity of VDAC in bilayers.

With some outer membrane patches (Tedeschi et al., 1987), the conductance also decreases with voltage in the negative range of potentials. However, with most patches the conductance increases reversibly and the time dependence is reproducible (Tedeschi et al., 1987; Kinnally et al., 1987). In these latter patches, voltage clamping with a negative potential above a patch-dependent threshold voltage results in a biphasic increase in conductance. A rapid increase is followed by a progressively larger conductance change. The kinetics of the conductance changes are consistent with an initial activation of channels followed by a voltage-dependent assembly of high-conductance channels. An assembly process for the second phase has been proposed (Kinnally et al., 1987) based on a number of observations. (a) Small voltage pulses superimposed on a minimal threshold voltage during the first phase produce a progressively larger conductance increase, consistent with a progressive assembly. (b) A second pulse above threshold induces a conductance increase which is greater for shorter time intervals between pulses, i.e., the system has a "memory" consist-

<sup>1</sup>The electrophysiological convention consists of reporting the polarity of the voltage clamp potentials in relation to the internal cell compartment. With this convention the polarity of the pipette would be expressed as the reverse of that of the internal compartment. In our previous two papers (Tedeschi, H., C. A. Mannella, and C. L. Bowman. 1987. *J. Membr. Biol.* 97:21–29; Kinnally, K. W., H. Tedeschi, and C. A. Mannella. 1987. *FEBS (Fed. Eur. Biochem. Soc.) Lett.* 226:83–87), we erroneously reported the pipette polarity following this convention rather than its actual polarity.

tent with reconstitution of a partially disassembled conductance state. These results are consistent with a process involving the assembly of a minimum of three subunits. (c) Although the time required to produce the second phase increase in conductance can be very long (several seconds at threshold voltages), recovery to a low conductance state monitored with a low background voltage can occur within 50 ms (Fig. 1), consistent with a partial disassembly collapsing the high conductance channel. (d) The temperature dependence of the increase in conductance is qualitatively very similar to that displayed by known channel assembly systems such as alamethicin (Boheim et al., 1980) and *S. aureus*  $\alpha$ -toxin (Ikigai and Nakae, 1984). (e) Finally, concanavalin A, which presumably favors aggregation of protein subunits, enhances the conductance increase.

The present study examines the kinetics of the conductance changes induced by negative voltages in outer mitochondrial membrane patches. The results can be fit to a model involving two separate but closely related voltage-dependent events: an opening of preexisting channels followed by the assembly of high-conductance channels from the activated subunits. This model suggests that assembly of the high-conductance channels requires from five to seven subunits.

## METHODS

### Experimental procedures

The preparation of the giant mitochondria and the production of large mitochondria in mice have been previously described (Bowman and

Tedeschi, 1983). Typically, mitochondria were suspended in 0.30 osmolar sucrose, 10 mM KCl, 5 mM Hepes, pH 7. The experiments were carried out at  $\sim 25^{\circ}\text{C}$ .

The electronics and experimental conditions have been presented previously (Tedeschi et al., 1987). Voltage clamp was maintained during the kinetic studies. Voltages are reported relative to the pipette.<sup>1</sup> The data were acquired and stored on floppy discs using an IBM-XT microcomputer with a model D/A 2801A board (Data Translation, Inc., Marlboro, MA) and software written by David Tieman of State University of New York at Albany. Conductances were computed from current and voltage recordings.

### Curve fitting and computer simulations

The parameters were evaluated by best fit using Lotus software (Lotus Development Corp., Cambridge, MA). The graphics of the program allow a direct comparison between the experimental curves and the curves generated by Eq. 2 (see below) when varying the values of the parameters (see Figs. 2 and 7).

To fit the experimental curves several parameters were first estimated from different regions of the curves (see details below). The rationale for the choice of the other parameters is explained below. Then the experimental curves were systematically compared with the curves computed after introducing small modifications of the parameters until a best fit was visually recognized. We found that adjustments of the parameters by as little as 5–10% had profound effects on the shape of the curves. To illustrate the reliability of the method, the values obtained by independent procedures departing from different initial values of the parameters are shown for one voltage in Figs. 3–6 by open or half open circles.

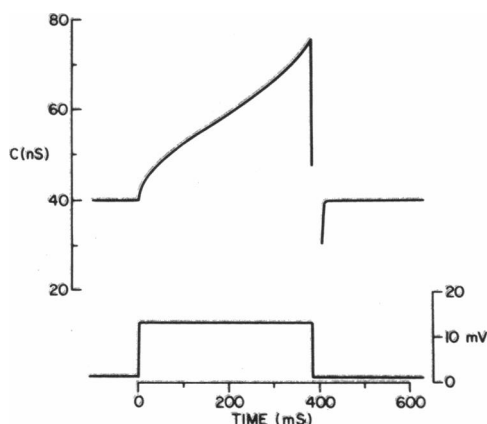


**FIGURE 1** Typical kinetics of voltage-induced conductance changes in a mitochondrial outer membrane patch. The outer membrane patch was voltage clamped at  $-1$  mV before a pulse of  $-13$  mV. Conductance was computed from current and voltage recorded every millisecond (1 KHz). The imposed voltages were negative in relation to the patch pipette. Increasing magnitude of negative voltages and outward current are represented in the figures as upward deflections.

## RESULTS AND COMPUTER SIMULATIONS

Typical kinetics of the biphasic conductance response to a negative voltage step are shown in Fig. 1. The delay of the onset of the second phase of the response is voltage dependent and can be several seconds long when applying a minimal threshold voltage, i.e., the lowest voltage necessary to elicit a biphasic response. Whereas the conductance increase of the second phase develops slowly, the recovery of the conductance to its original value occurs in  $<50$  ms as shown in Fig. 1. Capacitance corrections made improvements in the time resolution difficult and were not attempted. Hence the 50-ms recovery time can be considered an upper limit.

The voltage dependence of the biphasic conductance response, which differs from patch to patch (see Table 1), is illustrated by Fig. 2. The same patch was subjected to multiple voltage steps, and the conductance responses (computed from continual current and voltage recording) are represented by lines. Crosses represent computer simulations corresponding to the various voltage pulses for the model discussed below (the sudden leveling off of the experimental curves is due to saturation of the electronics). The biphasic kinetics suggest the presence of two processes. One is reflected in an initial rapid voltage-

TABLE 1 Parameters derived for experiments by procedure described in Appendix

Exp	mV	k	$\alpha$	Z	$\delta$	n
1	2.0	35 (40)	0.003	32.5	7	6
	2.5	40 (40)	0.037 (0.0048)	37.0 (380)	55 (1000)	8 (6)
	3.0	40 (40)	0.053 (0.0090)	37.0 (430)	290 (3000)	6 (6)
	3.5	40 (40)	0.050 (0.0075)	40.0 (450)	125 (1350)	6 (6)
	4.0	40 (40)	0.19 (0.030)	39.6 (440)	530 (5500)	6 (6)
	5.0	40 (40)	0.23 (0.0385)	45.0 (525)	755 (7400)	6 (6)
2	15.0	35	0.006	9.5	0.5	6
	16.0	35	0.021	11.0	4	10
3	25.0	—	—	2.3	0	6
	35.0	—	—	2.4	0.4	6
	40.0	0.013	—	2.6	0.9	6
	50.0	0.13	—	3.8	6	6
4 See Figs. 3–6.						

$C_x = 1$  nS/channel;  $C_y = 25$  nS/channel. Values in parentheses correspond to constants derived with  $C_x = 0.09$  ns/channel and  $C_y = 3$  ns/channel.

dependent increase in conductance which occurs even at very low voltages. The second voltage-dependent process is progressive and requires a minimum threshold voltage. One of the possible mechanisms to explain these results corresponds to an initial voltage activation and opening of channels of low conductance ( $X$ ) from a nonconducting population of precursors ( $Z$ ) (first process), followed by their conversion into ( $Y$ ) which instantaneously assemble into larger high conductance channels ( $Y$ )<sub>n</sub> (second pro-

cess) where  $n$  corresponds to the number of subunits forming the channel. This model predicts that an asymptotic conductance level should eventually be reached because there must be a finite number of activated subunits. Experimentally we have been able to follow the patch conductance over a limited range and we have not observed a leveling off. The expected asymptotic behavior was not observed even in cases in which the initial conductance changes are relatively small. This presumably reflects fewer  $X$  channels and so we would expect a steady state to be reached at a lower current level (at which the electronics would not saturate). We have therefore needed to incorporate in the model an additional feature, which produces an increase in  $X$  which is linear time. The possible physical event underlying this increase could correspond to an activation of precursors of  $X$ , distinct from  $Z$  and present in large amounts. Alternatively, the concentration of  $X$  could be increasing because of the electrophoretic migration of  $X$  into the patch from adjoining membrane regions. Cooperative effects in the assembly process could also account for this effect (see Discussion). The full model is represented in Eq. 1, a and b. In Eq. 1a,  $k$ ,  $\alpha$ ,  $\beta$ , and  $\delta$  are rate constants. In Eq. 1b,  $K_{eq}$  corresponds to the equilibrium constant for the formation of a channel ( $Y$ )<sub>n</sub> from  $Y$ , which is assumed to be at equilibrium.

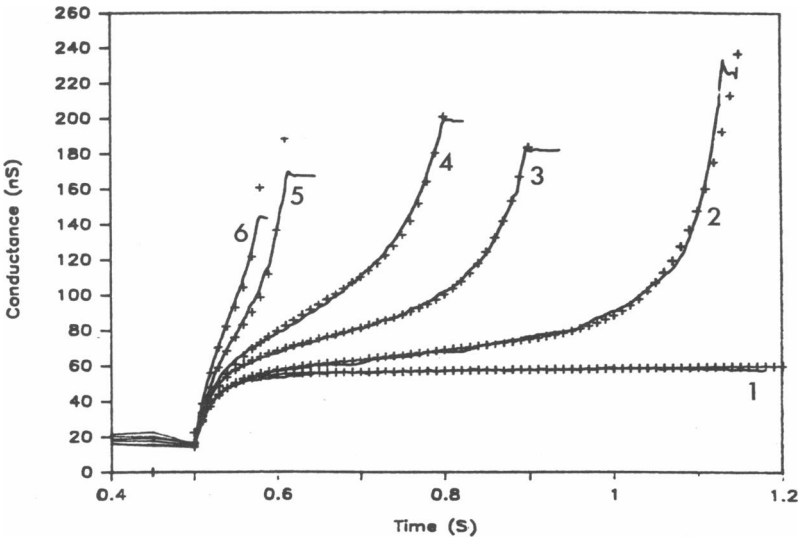
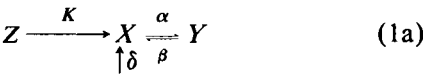


FIGURE 2 Conductance responses of one patch obtained with various clamping voltage pulses (see legend of Fig. 1). (Solid lines) Experimental results. (Crosses) A computer fit using Eq. 2 (in conjunction with Eqs. 6 and 7 of the Appendix) and the parameters listed in the Table 1 for experiment 1. The pulses were started at  $t = 0.5$  s. Curves 1–6 correspond to voltage pulses of 2, 2.5, 3.5, 3, 4, and 5 mV, respectively. Before the pulses, the conductances were computed from the currents with the potential clamped at 0.5 mV. Parts of curves 1–4 correspond to a moving average calculated over 20 ms.

$$n(Y) \xrightleftharpoons{K_{eq}} (Y)_n \quad (1b)$$

The corresponding rate equations and their solutions are shown in the Appendix. The total conductance ( $C$ ) assumes the form shown in Eq. 2, in which  $C_x = \gamma_x$ , the unit conductance of the  $X$  channels. On the other hand,  $C_y = K_{eq}(\gamma_y)$ , where  $\gamma_y$  is the unit conductance for the channel  $(Y)_n$  formed by  $n(Y)$ , where  $n$  corresponds to the number of  $Y$  subunits aggregating to form the final  $(Y)_n$  multimeric channel. The subunits  $Y$  do not conduct. The components of this equation are shown in detail in the Appendix. The portion of the model in which an assembly of subunits takes place to form a channel is the same as that originally proposed by Hodgkin and Huxley (1952) to explain delayed rectification of  $K^+$  channels. An aggregation model of gating has been considered previously by Bauman (1983).

$$C = C_x X(t) + C_y (Y)^n(t). \quad (2)$$

Fig. 2 contains a plot of the fit of the data based on Eq. 2 (see Appendix). The lines indicate the experimental results, and the computed fits are indicated by crosses.

In practice for all our fits  $C_x$  and  $C_y$  were chosen arbitrarily from various possible alternatives (see Discussion),  $k$ ,  $Z_0$ , and  $\delta$  were first calculated approximately from the experimental curves assuming  $\alpha = 0$ .  $Z_0$  was taken to correspond to the value estimated from the apparent asymptote reached in each curve for the first process. For the faster curves (e.g., curves 5 and 6 of Fig. 2) the inflection point was used for the initial estimates of  $Z_0$ .  $k$  was calculated from the initial slope of each curve.  $\delta$  was calculated from the slope of the curves were they deviated from the asymptote predicted on the assumption that  $\alpha = 0$ .  $\alpha$ ,  $\beta$ , and  $n$  were

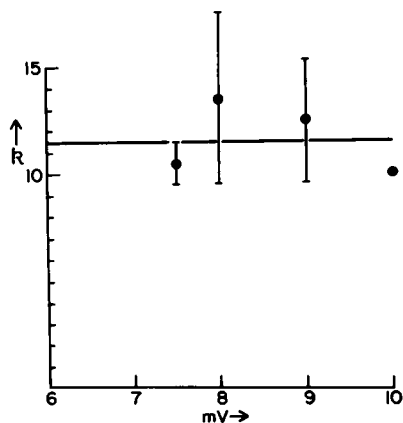


FIGURE 3 Dependence of  $k$  on voltage (see Eq. 1 and Appendix). The parameters were obtained by a computer simulation as shown in Fig. 7, from results obtained using the same patch. In Figs. 3–6 deviations represent SD with a minimum of four determinations.

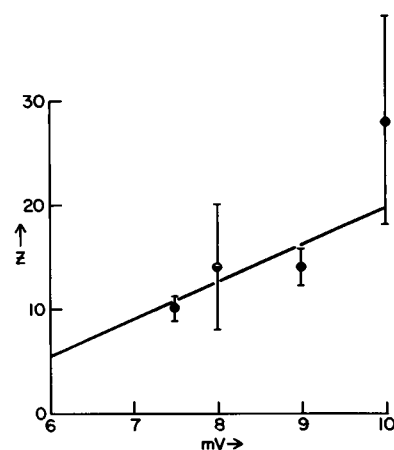


FIGURE 4 Dependence of  $Z$  on voltage (see legend of Fig. 3). (Open circle) An independent calculation of the parameter.

obtained approximately by trial and error with the restriction of the model that  $n \geq 3$ .

The parameters used in the fit of Fig. 2 are summarized in the Table 1 (experiment 1). The results suggest that  $k$ , the rate constant for the activation of single channels does not change with voltage. The number of subunits  $n$  needed to form a high-conductance channel corresponds to  $\sim 6$ . The values of  $Z$ , and the kinetic constants  $\alpha$  and  $\delta$  increase with voltage, whereas the constant  $\beta$  was found to be negligible. The values of  $Z$  and  $n$  and the kinetic constants obtained by best fit in a more complete experiment involving a minimum of four determinations per voltage for a single patch (experiment 4) are shown in Figs. 3–6. The open or half open circles represent a value obtained by an independent fit using different starting values for the parameters. The results support the conclusions that

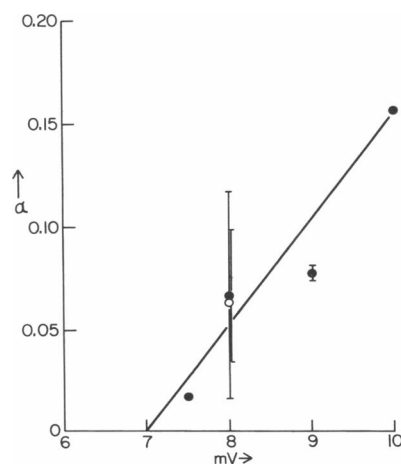


FIGURE 5 Dependence of  $\alpha$  on voltage (see legends of Figs. 3 and 4).

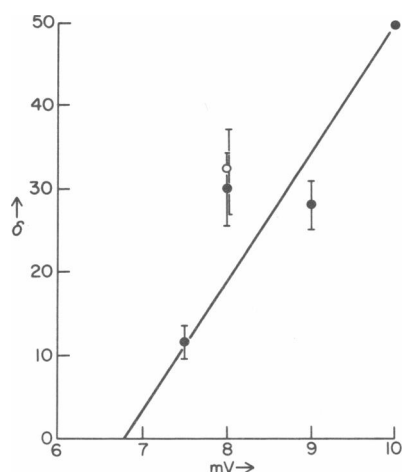


FIGURE 6 Dependence of  $\delta$  on voltage (see legends of Figs. 3 and 4).

$Z$  and the kinetic constants  $\alpha$  and  $\delta$ , but not  $k$  are voltage dependent. As summarized in Table 1, the voltage dependence and the actual values of the parameters differ with the individual patch. However, the values of  $n$  (usually 6) are the same from experiment to experiment.  $C_x$  and  $C_y$  taken in all cases as 1 and 25 nS/channel, respectively, were chosen arbitrarily from many possible values (see Discussion).

In the table we did not show  $k$  for experiment 3 in which the kinetics of the first phase are atypical. This experiment represents one of the very few patches

observed in which the conductance first decreases with voltage, a behavior we previously attributed to VDAC closing (Tedeschi et al., 1987).

A detailed example of the dependence of the kinetics on  $n$  is illustrated for one case in Figs. 7 and 8. The entire experimental curve and the points computed with  $n = 6$  (the crosses) are shown in Fig. 7. These experimental data are typical and correspond to one of the determination for 7.5 mV summarized in Figs. 3–6. Fig. 8 compares the experimental conductances calculated from the currents (ordinate) with the values computed using Eq. 2 (abscissa) for  $n = 4$ ,  $n = 5$ , and  $n = 8$ . As shown in the figure, conductance values computed with  $n = 5$  are very close to the experimental values, whereas calculations based on  $n = 8$  or 4 deviate significantly. The curves for  $n = 6$  and  $n = 7$  are indistinguishable from  $n = 5$ . Therefore for this fit  $n$  can be considered to correspond to  $6 \pm 1$ .

## DISCUSSION

### The models

The voltage-activated conductance increases observed in mitochondrial outer membrane patches are consistent with a two-phase model. In the first phase,  $X$  channels are activated from a precursor  $Z$ . There is a subsequent voltage-dependent assembly of  $Y$  subunits, formed from  $X$ , into a high conductance multimeric channel,  $(Y)_n$ , where  $n$  ranges from 5 to 7. These features of the model are represented in diagram 1 (Fig. 9). Because the

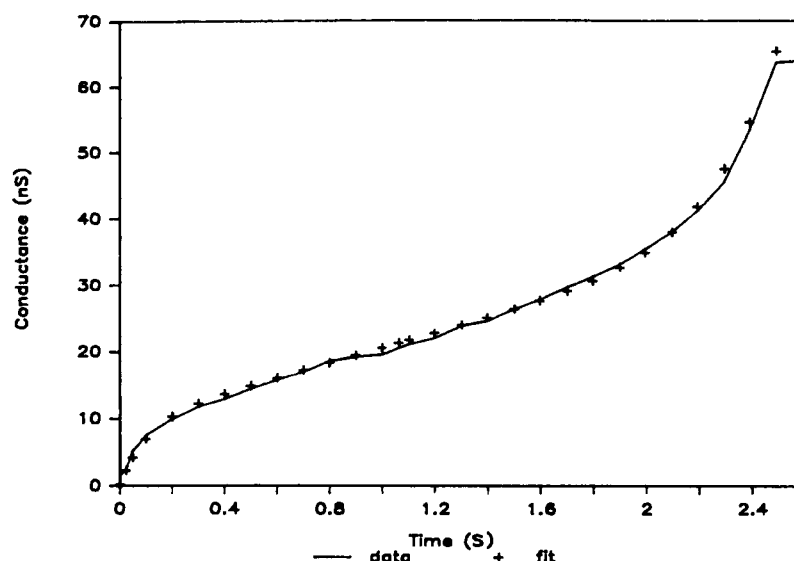


FIGURE 7 Observed conductances (solid line) and computer-simulated conductances (crosses) assuming  $n = 6$  during a voltage pulse of 7.5 mV. The conductance preceding the pulse was subtracted. The data was acquired by sampling at 1 KHz for 1 s and then at 0.125 KHz. Moving averages with an interval of 5 ms (before 1 s) and 32 ms (after 1 s) were used.

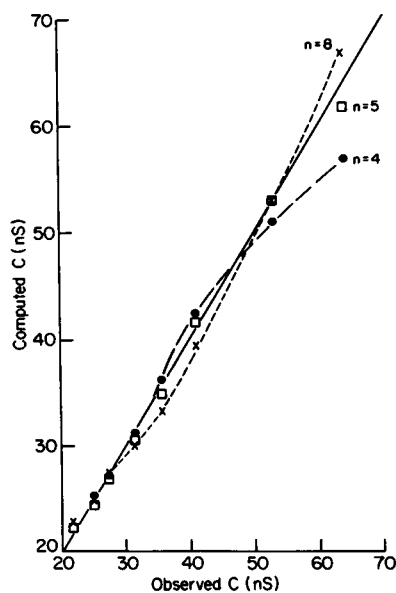


FIGURE 8 Comparison of the conductances computed from the observed currents to those simulated using Eq. 2 (in conjunction with Eqs. 6 and 7 of the Appendix), assuming as indicated  $n = 4$  (solid circles),  $n = 5$  (squares), or  $n = 8$  (crosses). Similar curves for  $n = 6$  and  $n = 7$  were indistinguishable from those for  $n = 5$ . Complete agreement between the observed conductances and those calculated from the model correspond to the solid line.

experimentally determined conductances have not been observed to reach a steady state, the model also includes a mechanism not shown in the figure by which  $X$  is produced by a voltage-dependent process from a large pool of precursors, independent of  $Z_0$  (Eq. 1).

A similar model proposes exactly the same sequence of events except that the  $X$  channels maintain their integrity as part of  $(Y)_n$ , i.e., their external surfaces remain intact and form the walls of channel  $Y$  (see diagram 2, Fig. 9). Although this model is expressed by a different set of equations (see Appendix), the computer simulations are very similar to those of the first model. Furthermore, the corresponding parameters computed for the two models do not differ significantly.

The models shown in Fig. 9 are for purposes of illustration only. They are in an arbitrary scale and are not intended to represent molecular mechanisms. Interestingly, the transition of  $X$  to  $(Y)_n$  in model 1 predicts an  $\sim 36$ -fold increase in unit conductance. In the special case for which  $K_{eq} = 1$ , for the  $Y$  to  $(Y)_n$  step,  $C_y$  is equal to  $\gamma_y$  (i.e.,  $C_y/C_x = \gamma_y/C_x$ ). In fact the best-fit ratio of  $C_y/C_x$  was found to range between 20 and 35 (see below). In contrast the expected increase in unit conductance is much smaller for model 2. In addition, model 2 is energetically unlikely without additional conformation changes in the subunits to form a new polar channel.

## Absence of steady state

The voltage-induced production of  $X$  from a presumed precursor other than  $Z$  has been invoked to explain the absence of a steady state. This production may involve a process of activation of units present in the patch. This can only be true if the pool of precursor is very large. The rate constant  $\delta$  could also be a reflection of cooperative behavior where the partial assembly of the subunits would facilitate the addition of others.

Another alternative is provided by the possibility that the two precursors are the same entity which increases in concentration in the patch by electrophoretic displacement from the surrounding membrane area. The electrophoretic migration of integral membrane proteins in the plane of the membrane has been demonstrated in the inner mitochondrial membrane (Sowers and Hackenbrock, 1981). In the patches, a component of the voltage may be in the plane of the membrane in the regions where the membrane parallels the walls of the patch pipette. The variability in the voltage dependence of  $\delta$  from patch to patch could then be accounted for by the variations in patch geometry.

In contrast to an activation phenomenon, an electrophoretic migration in the absence of a voltage gradient of opposite polarity should reverse only slowly. We have occasionally observed a persistence of a conductance higher than at the original level after prolonged pulses of large voltages (50–100 mV). Obviously resolution of this question requires additional experiments.

## $C_x$ and $C_y$

$C_x$  and  $C_y$  correspond respectively to the conductance per  $X$  channel and assuming  $K_{eq} = 1$ , per  $(Y)_n$  channel. The

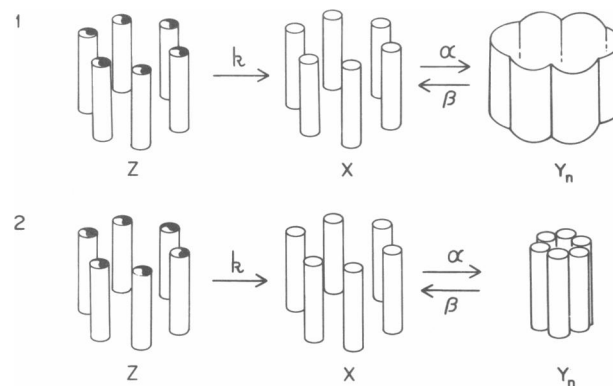


FIGURE 9 Schematic representation of two models to account for the assembly of high-conductance channels (see Discussion). The cylinders represent open channels; the solid portions represent partially closed gates. The activated  $X$ , subunits  $Y$ , are not shown. The scale is arbitrary and the diagrams do not depict molecular configurations.

values were taken arbitrarily to be 1 nS/channel and 25 nS/channel, respectively. As long as the ratio of  $C_y/C_x$  remains approximately the same, other values produce similar fits. Although the various parameters would have different values, the voltage dependence still remains and the value of  $n$  (i.e., 5–7) does not change. For a  $C_x$  of 1 nS per channel the total number of  $X$  channels per patch would be as low as 10–40.

The values chosen for  $C_y$  and  $C_x$  are very high compared with that of known high-conductance channels. For example, that of VDAC in 10 mM KCl would correspond to 0.045 nS. Therefore it becomes important to examine other alternatives. We have found in many cases that in the absence of the second phase, at steady state the conductances of the first phase are approximately twice those before the voltage pulse. We have attributed the conductances preceding the voltage pulses to VDAC (Tedeschi et al., 1987). If we were to assume that  $X$  corresponds to activated VDAC, it follows that  $C_x$  should be approximately twice that of VDAC, i.e., under these conditions ~0.090 nS. For this case  $X$  would correspond to a very large number. In the experiment of Fig. 2 it would be >400. The simulation using these values are approximately the same as those shown in Fig. 2, and the corresponding constants are those shown in Table 1, experiment 1 in parentheses.

### Variability from patch to patch

The variability of  $k$ ,  $\alpha$  and  $Z_0$  from patch to patch is considerable. As already mentioned,  $\delta$  is likely to depend on the geometry of the patch which will be variable in each case. Because  $Z_0$  corresponds to the concentration of a precursor, its variability is also not surprising. We have found that the base conductance (i.e., close to 0 mV) is different from patch to patch. We take this to mean that the concentration of  $Z$  channels differs in different patches. The possible explanation that the degree of patch sealing differs (i.e., the leak pathway varies) is not likely because the voltage-dependent proportion of the total conductance is approximately the same in every patch in the voltage range at which the channels partially close (Tedeschi et al., 1987) and approximately the same than in VDAC incorporated in bilayers.

We think that the variability of the constants  $k$  and  $\alpha$  may arise from an endogenous modulator of the voltage sensitivity of the precursor channel. Synthetic polyanions have been shown to alter the rate and extent of closing of VDAC (Mangan and Colombini, 1987; Colombini et al., 1987). Holden and Colombini (1988) have recently reported the presence of an endogenous mitochondrial protein which also increases the voltage-induced rate and extent of closing of VDAC. In their experiments the rate of closing was shown to increase >10-fold in the presence

of the factor. Furthermore, the rate of reopening is decreased by three orders of magnitude and the voltages at which the VDAC reopen is decreased dramatically. They propose a physiological modulator role for this protein. We have previously presented evidence of such factor in outer mitochondrial membrane and showed that its presence probably differed from patch to patch (Tedeschi et al., 1987). This conclusion was based on the different effects of a synthetic polyanion on patch conductance. In patches in which voltage sensitivity was already maximal, the polyanion was totally ineffective. However, the polyanion produced a maximal effect when added to patches which were less responsive to voltage. Our earlier results also indicated that the polyanion increased the steepness of the voltage-dependent conductance increased observed in the negative range of voltage of the present experiments (e.g., see Tedeschi et al., 1987, Fig. 7). We think that the polyanion may mimic the natural modulator in this case as well.

### The constant $\alpha$

The transition from  $X$  to  $Y$  (the second reaction in Eq. 1) is likely to correspond to a movement of  $X$  to a location favoring its aggregation such as transmembrane movement. This is one of the possibilities first suggested by Hodgkin and Huxley (1952) for a similar model. There is experimental evidence for such voltage-induced translocations across lipid bilayers in the case of the asialoglycoprotein receptor (Blumenthal et al., 1980). In our model the unexpected temperature dependence of the second phase conductance increase previously described (Kinnally et al., 1987) is likely to correspond to changes in either  $\alpha$  or  $K_{eq}$  brought about by lipid phase transitions.

### Are phase 1 channels precursors of phase 2 channels?

The models presented in this paper presume that the second change in conductance results from the assembly of channels formed or activated in the first phase. The first phase increase can take place alone. However, as long as the voltage pulses are above threshold, the second phase seems to correlate in rate to the changes of the first. These observations and our simulations of the kinetics, however, do not preclude an entirely different model explaining the results with two or three independent mechanisms.

### Nature of channel protein(s)

Previous studies of others have found 8 to 10 separate polypeptide bands in outer mitochondrial membranes of *Neurospora* (Freitag et al., 1982) and 11 in rat liver

mitochondria (Melnick et al., 1973) using SDS-PAGE. In addition, the VDAC polypeptide represents only ~20% of the outer membrane protein of *Neurospora* mitochondria (Freitag et al., 1983). It is therefore entirely possible that the effects described here correspond to channels distinct from VDAC. However, the tendency of VDAC to associate in groups of six (Mannella, 1987) raises the possibility of their involvement in this putative assembly process (for which  $n = 6 \pm 1$ ). In addition VDAC has a known affinity for concanavalin A and we have shown a facilitation of phase 2 conductance increases by this lectin (Kinnally et al., 1987).

If the phenomenon described here corresponds to a novel behavior of VDAC, why have studies using bilayers not revealed it? There are several possible explanations. Bilayer studies are generally carried out at high ionic strength which may decrease electrostatic interactions involved in aggregation. Our studies were carried out at relatively low ionic strength. As previously discussed (Tedeschi et al., 1987), the concentration of VDAC is much different. In our patches there should be several hundred or a few thousand per square micrometer, whereas in the bilayer there should be no more than a few hundred per square millimeter. There is evidence of cooperative behavior with clustering at least in the case of the acetylcholine channel (Young and Poo, 1983). In addition as already mentioned there are many other proteins present in the native outer membrane which could alter the behavior of the VDAC.

## APPENDIX

For the model of diagram 1, the conductance can be calculated from Eq. 2 (see text). Eqs. 3–5 are rate equations for  $Z$ ,  $X$ , and  $Y$ .  $Y$  and  $X$  are represented by Eqs. 6 and 7, derived by appropriate manipulations and integrations of Eqs. 3–5, assuming that at  $t = 0$ ,  $X$  and  $Y = 0$ , and  $Z = Z_0$ .

$$\frac{dZ}{dt} = -kZ \quad (3)$$

$$\frac{dX}{dt} = kZ + \delta - \alpha X + \beta Y \quad (4)$$

$$\frac{dY}{dt} = \alpha X - \beta Y \quad (5)$$

$$Y = \frac{\alpha Z_0}{(\alpha + \beta)} [1 - e^{-(\alpha + \beta)t}] - \frac{\alpha Z_0}{(\alpha + \beta - k)} [e^{-kt} - e^{-(\alpha + \beta)t}] + \frac{\alpha \delta}{(\alpha + \beta)^2} \{[(\alpha + \beta)t - 1] + e^{-(\alpha + \beta)t}\} \quad (6)$$

$$X = Z_0(1 - e^{-kt}) + \delta t - \frac{\alpha Z_0}{(\alpha + \beta)} [1 - e^{-(\alpha + \beta)t}] + \frac{\alpha Z_0}{(\alpha + \beta - k)} [e^{-kt} - e^{-(\alpha + \beta)t}] - \frac{\alpha \delta}{(\alpha + \beta)^2} \{[(\alpha + \beta)t - 1] + e^{-(\alpha + \beta)t}\} \quad (7)$$

For the model of diagram 2 the Eqs. 3–6 apply. However,  $C_x$  denotes the conductance coefficient for the  $X$  channel whether alone or when forming channel  $Y$  and  $X$  is represented by Eq. 8.

$$X = \delta t + Z_0(1 - e^{-kt}). \quad (8)$$

David Tieman (Department of Biological Sciences, State University of New York at Albany) guided us through the use of the microcomputers and developed some of the software.

This study was supported in part by ONR grant N0001485-K-0681 (H. Tedeschi), and National Science Foundation grants DMB-8613702 (C. Mannella) and DMR-8515519 (H. Frisch).

Received for publication 17 October 1988 and in final form 27 January 1989.

## REFERENCES

- Bauman, G. 1983. Stochastic modeling of the aggregation-gating site. *In* Structure and Function in Excitable Cells. D. C. Chang, L. Tasaki, W. J. Adelman, Jr., and H. R. Leuchtag, editors. Plenum Publishing Corp., New York. 255–271.
- Benz, R. 1985. Porin from bacterial and mitochondrial outer membranes. *CRC Crit. Rev. Biochem.* 19:145–190.
- Blumenthal, R., R. D. Klausner, and J. N. Weinstein. 1980. Voltage-dependent translocation of the asialoglycoprotein receptor across lipid membranes. *Nature (Lond.)* 288:333–338.
- Boheim, G., W. Hanke, and H. Eibl. 1980. Lipid phase transition in planar bilayer membrane and its effect on carrier- and pore-mediated ion transport. *Proc. Natl. Acad. Sci. USA* 77:3403–3407.
- Bowman, C. L., and H. Tedeschi. 1983. Kinetics of lucifer yellow CH efflux in giant mitochondria. *Biochem. Biophys. Acta* 731:260–266.
- Colombini, M. 1985. Voltage gating in VDAC. Toward a molecular mechanism. *In* Ion Channel Reconstitution. C. Miller, editor. Plenum Publishing Corp., New York. 533–552.
- Colombini, M., C. L. Yeung, J. Tung, and T. Konig. 1987. The mitochondrial outer membrane channel, VDAC, is regulated by a synthetic polyanion. *Biochim. Biophys. Acta* 905:279–286.
- DePinto, V., O. Ludwig, J. Krause, R. Benz, and F. Palmieri. 1987. Porin pores of mitochondrial outer membranes from high and low eukaryotic cells: biochemical and biophysical characterization. *Biochim. Biophys. Acta* 894:109–119.
- Doring, C., and M. Colombini. 1985. Voltage dependence and ion selectivity of mitochondrial channel, VDAC, are modified by succinic anhydride. *J. Membr. Biol.* 83:81–86.
- Freitag, H., W. Neupert, and R. Benz. 1982. Purification and charac-



- terization of a pore protein of the outer mitochondrial membrane from *Neurospora crassa*. *Eur. J. Biochem.* 123:629–636.
- Freitag, H., R. Benz, and W. Neupert. 1983. Isolation and properties of porin of the outer mitochondrial membrane of *Neurospora crassa*. *Methods Enzymol.* 97:286–294.
- Hodgkin, A. L., and A. F. Huxley. 1952. A quantitative description of membrane current and its application to conduction and excitation in nerve. *J. Physiol (Lond.)*. 117:500–544.
- Holden, M. J., and M. Colombini. 1988. The mitochondrial outer membrane channel, VDAC, is modulated by a soluble protein. *FEBS (Fed. Eur. Biochem. Soc.) Lett.* 241:105–109.
- Ikigai, H., and T. Nakae. 1984. The rate assay of alpha-toxin assembly in membrane. *FEMS (Fed. Eur. Microbiol. Soc.) Lett.* 24:319–322.
- Kinnally, K. W., H. Tedeschi, and C. A. Mannella. 1987. Evidence for a novel voltage-activated channel in the outer mitochondrial membrane. *FEBS (Fed. Eur. Biochem. Soc.) Lett.* 226:83–87.
- Mangan, P. S., and M. Colombini. 1987. Ultrasteep voltage dependence in a membrane channel. *Proc. Natl. Acad. Sci. USA.* 84:4896–4900.
- Mannella, C. A. 1987. Electron microscopy and image analysis of the mitochondrial outer membrane channel, VDAC. *J. Bioenerg. Bio-membr.* 19:329–340.
- Melnick, T. L., H. M. Tinberg, H. Maguire, and L. Packer. 1973. Studies of mitochondrial proteins. I. Separation and characterization by polyacrylamide gel electrophoresis. *Biochim. Biophys. Acta.* 311:230–241.
- Sorgato, M. C., B. U. Keller, and W. Stühmer. 1987. Patch-clamping of the inner mitochondrial membrane reveals a voltage-dependent ion channel. *Nature (Lond.)*. 330:498–500.
- Sowers, A. E., and C. R. Hackenbrock. 1981. Rate of lateral diffusion of intramembrane particles: measurement by electrophoretic displacement and rerandomization. *Proc. Natl. Acad. Sci. USA.* 78:6246–6250.
- Tedeschi, H., C. A. Mannella, and C. L. Bowman. 1987. Patch clamping the outer mitochondrial membrane. *J. Membr. Biol.* 97:21–29.
- Thieffry, M., J.-P. Chich, D. Goldschmidt, and J.-P. Henry. 1988. Incorporation in lipid bilayers of a large conductance cationic channel from mitochondrial membranes. *EMBO (Eur. Mol. Biol. Organ.) J.* 7:1449–1454.
- Young, S. H. and M.-M. Poo. 1983. Topographical rearrangement of acetylcholine receptors alters channel kinetics. *Nature (Lond.)*. 304:161–163.